JCTC Journal of Chemical Theory and Computation

Article

pubs.acs.org/JCTC

Inner Space Perturbation Theory in Matrix Product States: Replacing Expensive Iterative Diagonalization

Jiajun Ren,[†] Yuanping Yi,[‡] and Zhigang Shuai*,[†]

[†]MOE Key Laboratory of Organic OptoElectronics and Molecular Engineering, Department of Chemistry, Tsinghua University, Beijing 100084, People's Republic of China

[‡]Key Laboratory of Organic Solids, Beijing National Laboratory for Molecular Science (BNLMS), Institute of Chemistry, Chinese Academy of Sciences, Beijing 100190, People's Republic of China

ABSTRACT: We propose an inner space perturbation theory (isPT) to replace the expensive iterative diagonalization in the standard density matrix renormalization group theory (DMRG). The retained reduced density matrix eigenstates are partitioned into the active and secondary space. The first-order wave function and the second- and third-order energies are easily computed by using one step Davidson iteration. Our formulation has several advantages including (i) keeping a balance between the efficiency and accuracy, (ii) capturing more entanglement with the same amount of computational time, (iii) recovery of the standard DMRG when all the basis states belong to the active space. Numerical examples for the polyacenes and periacene show that the efficiency gain is considerable and the accuracy loss due to the perturbation treatment is very small, when half of the total basis states belong to the active space. Moreover, the perturbation calculations converge in all our numerical examples.

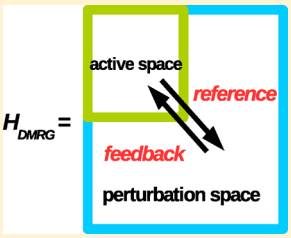

1. INTRODUCTION

Density matrix renormalization group theory (DMRG)[1] or its modern name matrix product states (MPS) has been widely accepted as a powerful wave function ansatz to treat strong correlation system in quantum chemistry field, especially in those static correlation dominant systems. It has been successfully used to calculate the electronic structure of the π conjugated systems,[2−4] transition metals,[5−7] etc. With the rapid development of computer performance,[8] the state-of-the-art quantum chemistry DMRG (QC-DMRG) program[9−11] nowadays can treat up to one hundred active orbitals which largely surpasses the complete active space self-consistent field method (CASSCF).[12] However, the accuracy of DMRG decreases when going from one-dimensional system to two- or three-dimensional systems with the same number of retained basis states (M), because of the so-called area law,[13] and in general, quantum chemistry is a three-dimensional problem. Several methods were developed to solve this problem. Wouters et al.[14] and Haegeman et al.[15] explored correction in the tangent space of MPS with configuration interaction method (CI-MPS) or random phase approximation (RPA-MPS). Murg et al.[16] and Nakatani et al.[17] extended one dimension MPS structure to tree tensor network states (TTNS). TTNS can capture more entanglement with the same M value in principle, because the distance between two entangled orbitals is $\log(N)$ in TTNS structure. The dimension of reduced Hilbert space, to be diagonalized in each optimization step, is $O(M^Z)$ approximately, where Z is the number of tree branches. Though the Hamiltonian is never explicitly constructed, TTNS is still much more expensive than MPS due to the calculation of $H\cdot C$ in the iterative diagonalization algorithm, such as Davidson diagonalization algorithm.[18] Thus, staying in the same MPS framework and increasing the M value is an appropriate choice. A typical QC-DMRG calculation uses M = 1000−10 000. The main cost of MPS algorithm is $O(M^3)$, coming from the matrix−matrix product in calculating $H\cdot C$. According to the numerical results reported by Chan[19] and our results shown below, the time cost of the Davidson diagonalization process consists of nearly 90% of the total, even with the massively parallel algorithm. This is the most important restriction for M to be several thousand. Therefore, if we can use a smaller M to achieve the same accuracy, DMRG will be more efficient. In this work, we propose a methodology to explore a larger M space to reach higher accuracy without increasing the cost.

In the classic quantum chemistry theories, the single reference perturbation theory (PT), like Møller−Plesset PT[20] performs well if the Hatree-Fock single determinant is a good starting point. The multireference PT, like the complete active space perturbation theory (CASPT),[21] performs well if the CAS space can treat static correlation correctly. This indicates that if the reference is qualitatively correct, PT could be a suitable choice to balance the accuracy and efficiency. Since DMRG always adapts the many body basis states and thus restricts the low energy states in a proper small space, even a small M can obtain a qualitatively correct result. This valuable inherent nature of DMRG provides us an opportunity to treat a small M space as a reference and apply perturbation theory in a large M space on this good reference. To the best of our knowledge, this feature has not been explored yet. Herein, we propose a new formulation called DMRG inner space perturbation theory (DMRG-isPT) to replace the expensive

Received: July 13, 2016
Published: September 6, 2016

DOI: 10.1021/acs.jctc.6b00696
J. Chem. Theory Comput. 2016, 12, 4871−4878

exact diagonalization procedure in each local matrix optimization step in order to achieve high efficiency and maintain accuracy at the same time. The word "inner" is used to distinguish this formulation from the earlier developed DMRG perturbation method, such as DMRG-CASPT,[22] MPS-PT,[23] and DMRG-NEVPT,[24] which are developed to incorporate dynamical correlation due to the frozen core orbitals and the unoccupied secondary orbitals.

The rest of the paper is organized as follows. In the Theory section, we describe this DMRG-isPT formulation and algorithm. After this, we show two benchmark calculations, one on the acene series and the other on a simple two-dimensional molecule (5,3)-periacene. Finally, the conclusion is given.

2. THEORY

2.1. DMRG Theory. DMRG theory and its algorithm have been described in detail in many other excellent papers.[19,25−27] Here, to be self-contained, we briefly review the most essential parts of DMRG in MPS language.

Any wave function based on n one electron orbital $|\sigma_1\rangle$, $|\sigma_2\rangle$, ···, $|\sigma_n\rangle$ can be exactly parametrized as

$$|\Psi\rangle = C_{\sigma_1\sigma_2\cdots\sigma_n}|\sigma_1\sigma_2\cdots\sigma_n\rangle = \sum_{a_1,a_2,\cdots,a_{n-1}} A^{\sigma_1}_{a_1} A^{\sigma_2}_{a_1 a_2}\cdots A^{\sigma_n}_{a_{n-1}}|\sigma_1\sigma_2\cdots\sigma_n\rangle \quad (1)$$

a_i is called the virtual bond index and σ_i is called the physical index. The final ansatz is called MPS. This coefficient is decomposed by $n-1$ successive singular value decomposition (SVD).

$$C_{ab} = \sum_d U_{ad} S_{dd} V^{\dagger}_{db} \quad (2)$$

S is a diagonal matrix and its dimension equals min $\{a, b\}$. If we do not cut off the virtual bond dimension, the dimension of matrix A grows up exponentially. That will be 1×4, 4×4^2,···, $4^{n/2-1}\times 4^{n/2}$, $4^{n/2}\times 4^{n/2-1}$,···, 4×1, if n is even. Under the variational principle, optimizing all matrices at one time is a difficult task, because it is a set of nonlinear equations. One-site DMRG algorithm optimizes each matrix successively to reach an energy minimum. At each optimization step, the orbitals are partitioned into two subsystems, A and B, and then an eigenvalue equation is solved in a space spanned by the direct product of A and B subsystem basis states $|l\rangle_A \otimes |r\rangle_B$.

$$\sum_{l'r'} H_{lrl'r}\psi_{l'r'} = E\psi_{lr} \quad (3)$$

The Hamiltonian H is a huge matrix and the dimension of H is $O(M^2)$. Iterative diagonalization algorithm like Davidson diagonalization algorithm is used to solve this eigenvalue equation. At each Davidson iteration, $H\cdot\psi$ is calculated and H is constructed directly and implicitly with composite operator algorithm.[28] This is the key point of QC-DMRG algorithm.

$$H\cdot\psi = \sum_{l'r'AB} O[A]_{ll'} \otimes O[B]_{rr'}\psi_{l'r'} \quad (4)$$

DMRG theory constrains the dimension of each matrix up to M. If a_i is larger than M, DMRG uses SVD algorithm or diagonalizes the reduced density matrix to select the largest M singular value components. These two methods are the same. In fact, the information on wave function $|\psi\rangle$ is compressed, and the compressed $|\tilde{\psi}\rangle$ is selected to minimize the norm $||\psi\rangle - |\tilde{\psi}\rangle|^2$ with a limited number of basis states, thus

$$|\tilde{\psi}\rangle = \sum_{d=1}^{M} s_d|d\rangle_A|d\rangle_B \quad (5)$$

$s_1, s_2, \cdots, s_M$ are the largest M singular values in the whole set. The $|d\rangle_A$, $|d\rangle_B$ are the new basis states in subsystem A and B. The discarded weight is defined as $\epsilon = 1-\sum_{d=1}^{M} s_d$, which is used to measure the accuracy of DMRG calculation. If the singular values are in descending order, the most essential space is in the top-left corner of the whole space. Thus, we can exactly diagonalize in this corner space and add perturbation when considering the neglected outer space.

2.2. Many Body Perturbation Theory. Following the Rayleigh−Schrödinger perturbation theory (RSPT)

$$\hat{H} = \hat{H}_0 + \hat{U} \quad (6)$$

$$\hat{H}_0|i^{(0)}\rangle = E_i^{(0)}|i^{(0)}\rangle \quad (7)$$

Here, $\hat{H}_0$, $E_i^{(0)}$, and $|i^{(0)}\rangle$ are, respectively, the zeroth-order Hamiltonian and the zeroth-order energy and wave function of the ith state. $\hat{U}$ is the perturbation. Then if we consider the zeroth order wave function of the ith state $|i^{(0)}\rangle$, the first-order wave function, the first-order and second-order energies are

$$|i^{(1)}\rangle = -\hat{P}(\hat{H}_0 - E_i^{(0)})^{-1}\hat{P}\hat{U}|i^{(0)}\rangle \quad (8)$$

$$E_i^{(1)} = \langle i^{(0)}|\hat{U}|i^{(0)}\rangle \quad (9)$$

$$E_i^{(2)} = \langle i^{(0)}|\hat{U}|i^{(1)}\rangle \quad (10)$$

Here, $\hat{P}$ is a projection operator that projects a vector to the space orthogonal to $|i^{(0)}\rangle$

$$\hat{P} = 1 - |i^{(0)}\rangle\langle i^{(0)}| \quad (11)$$

According to Wigner's $2n+1$ rule, the third order energy can also be calculated from the first-order wave function

$$E_i^{(3)} = \langle i^{(1)}|\hat{U} - E_i^{(1)}|i^{(1)}\rangle \quad (12)$$

The more detailed derivation of RSPT can be found in ref 29.

2.3. DMRG-isPT2/3 Method. We only consider the first order wave function and up to the third order energy in this work. We call them DMRG-isPT2 and DMRG-isPT3. In the following derivation, M_p represents the number of subsystem basis states which are retained in each DMRG sweep. In these M_p basis, the first m basis states belong to the active space. So in the two-site MPS algorithm, the dimension of the active space is $16m^2$, and the dimension of the whole space is $16M_p^2$. In Figure 1, the whole Hamiltonian is represented in matrix form and the small top-left square is the active space Hamiltonian. The basis states $|\psi\rangle$ are classified into three groups. $|\psi_{i,j,k,\ldots}\rangle$ refers to the basis state that is exact eigenvector in the CAS space; $|\psi_{p,q,r,\ldots}\rangle$ refers to the basis state that is in the CAS space but orthogonal to $|\psi_{i,j,k,\ldots}\rangle$; $|\psi_{a,b,c,\ldots}\rangle$ refers to the basis state that is outside the CAS space.

First, we need to define the zeroth-order Hamiltonian. Since we exactly diagonalize the active space Hamiltonian, it is very straightforward to treat the diagonal elements of the whole Hamiltonian as $\hat{H}_0$, which is the black part shown in Figure 1. In this partition scheme, $|\psi_{i,j,k,\ldots}\rangle = \sum_{lr} C_{lr}^{i,j,k,\ldots}|lr\rangle$ and $|\psi_{a,b,c,\ldots}\rangle = |lr\rangle_{a,b,c,\ldots}$ are eigenvectors of $\hat{H}_0$. But $|\psi_{p,q,r,\ldots}\rangle$ is not. Here, C_{lr}^{i} is

DOI: 10.1021/acs.jctc.6b00696
J. Chem. Theory Comput. 2016, 12, 4871−4878

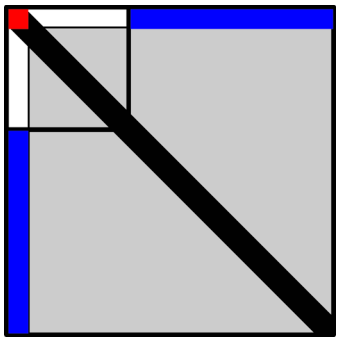

Figure 1. Hamiltonian matrix. Different colors represent the active space eigenvalue (red), diagonal element (black), first-order interaction element (blue), zero element (white), and nonzero element (gray).

the coefficient of the ith eigenstate in the active space expanded in the whole space, so $C_{lr} \equiv 0$ if $|lr\rangle \notin$ CAS.

We consider the zeroth-order wave function of the ith state $|i^{(0)}\rangle$. Apparently

$$E_i^{(1)} = \langle \psi_i^{(0)} | \hat{U} | \psi_i^{(0)} \rangle = 0 \tag{13}$$

As in the CASPT theory, $|\psi_{i,j,k,\ldots}^{(0)}\rangle$ are exact eigenvectors in the CAS space, so

$$\langle \psi_i^{(0)} | \hat{U} | \psi_p \rangle = \langle \psi_i^{(0)} | \hat{H} - \hat{H}_0 | \psi_p \rangle = 0 \tag{14}$$

Then, according to eqs 8 and 10, the first-order wave function correction and the second-order energy correction are

$$|\psi_i^{(1)}\rangle = \sum_{a \notin \mathrm{CAS}} \frac{U_{ai}}{E_i^{(0)} - E_a^{(0)}} |\psi_a^{(0)}\rangle \tag{15}$$

$$E_i^{(2)} = \sum_{a \notin \mathrm{CAS}} \frac{|U_{ai}|^2}{E_i^{(0)} - E_a^{(0)}} \tag{16}$$

The matrix element $U_{ai} = \langle \psi_a^{(0)} | \hat{U} | \psi_i^{(0)} \rangle$ is the blue part of H shown in Figure 1 and can be expressed as

$$\begin{aligned} U_{ai} &= \langle \psi_a^{(0)} | \hat{H} - \hat{H}_0 | \psi_i^{(0)} \rangle \\ &= \sum_{lr} \langle l'_a r'_a | \hat{H} C_{lr}^i | lr \rangle \\ &= C'^{\,i}_{l'_a r'_a} \end{aligned} \tag{17}$$

Each matrix element U_{ai} corresponds to one component in $C' = HC$. Then, all matrix elements can be calculated in just one step Davidson iteration efficiently.

The third-order energy correction is a little bit complicated. We define an intermediate coefficient

$$C_a^i = \frac{U_{ai}}{E_i^{(0)} - E_a^{(0)}} \tag{18}$$

According to eq 12

$$\begin{aligned} E_i^{(3)} &= \sum_{a,b \notin \mathrm{CAS}} C_b^i \langle \psi_b^{(0)} | \hat{U} C_a^i | \psi_a^{(0)} \rangle \\ &= \sum_{b \notin \mathrm{CAS}} C_b^i \Big(\sum_{a \notin \mathrm{CAS}} \langle \psi_b^{(0)} | \hat{H} C_a^i | \psi_a^{(0)} \rangle - H_{0bb} C_b^i \Big) \end{aligned} \tag{19}$$

As the second-order energy correction algorithm, each matrix element of the first term in parentheses is just one component of $C' = HC$, so we still can calculate all matrix elements in one Davidson iteration. $H_{0\,bb}$ in the second term is the diagonal element of H.

In DMRG-isPT2/3, "small space diagonalization + large space perturbation" algorithm is adopted to replace the standard large space diagonalization algorithm in each local matrix optimization step. The sweep process is summarized as follows:

(i) The subsystem is constructed that one is enlarged by combining the neighbor site and the other is shrinked by one site. The dimension of each subsystem is $4M_p$.

(ii) The direct product of the first m basis states of each subsystem spans an active space. The active space Hamiltonian (dimension is $16m^2$) is diagonalized to obtain the zeroth order eigenstate $|\psi_{i,j,k,\ldots}^{(0)}\rangle$ and energy $E_{i,j,k,\ldots}^{(0)}$.

(iii) Based on eqs 15, 16, and 19, we calculate the first-order wave function and second- and third-order energies in the whole space (dimension is $16M_p{}^2$).

(iv) With the first order corrected wave function, we select the largest M_p singular value components and transform the subsystem basis states from $4M_p$ to M_p by using SVD algorithm. The first m basis states, which correspond to the largest m singular values, are defined as the active basis states. With this decimation, we can start a new iteration at step i.

DMRG-isPT is in principle a multireference perturbation method and the perturbation space can feed back to the active space iteratively. Other than depending on one single parameter M, the accuracy of DMRG-isPT depends on two parameters (m, M_p). The upper limit of DMRG-isPT is M = M_p standard DMRG, because in each optimization step, the wave function is more accurate and then the retained basis states are adapted more properly. Apparently, when all basis states belong to the active space ($m = M_p$), DMRG-isPT recovers to the standard DMRG. Thus, the advantage of DMRG-isPT is that it is controllable in keeping a balance between the accuracy and efficiency. And with the same amount of computational time, it can treat a larger M_p and incorporate entanglement from the larger space ($M_p > M$) than what the standard DMRG can treat. This space, though treated at perturbation level, is vital to obtain a quantitatively correct result. Because in the two and three-dimensional systems, the discarded weight is not so small, completely neglecting these discarded basis states is dangerous. Including some of them at perturbation level is a reasonable and efficient way. Moreover, we can do exact diagonalization in the large space to check whether the perturbation treatment works or not and update the wave function more properly at the middle of each sweep (when the variational space is the largest in most cases). If the system is large enough, the time cost of this last step large space diagonalization will not be dominant.

We can analyze the efficiency gain approximately now. In each diagonalization step of the standard QC-DMRG algorithm, the time cost is $O(nM_p{}^3k^2)$, where n is the number of Davidson iterations it takes. The time cost of calculating the second order energy is $O((M_p{}^2m + M_pm^2)k^2)$, because the active space coefficient C_{lr}^i in eq 17 is just a $m \times m$ matrix. The time cost of calculating the third order energy is the same as one step QC-DMRG $O(M_p{}^3k^2)$. However, since the third order

DOI: 10.1021/acs.jctc.6b00696
J. Chem. Theory Comput. 2016, 12, 4871−4878

energy correction does not contribute to the optimization process, we can calculate it only at the middle in each sweep iteration, so it is for free. Therefore, in the DMRG-isPT algorithm, the total time cost is $O(nm^3k^2 + M_p{}^2mk^2 + M_pm^2k^2)$. We assume that the prefactor is the same and the number of Davidson iterations n is not related to the dimension of Hamiltonian. Then, the ideal speedup is

$$\text{speedup} = \frac{n \times M_p{}^3k^2}{n \times m^3k^2 + M_p{}^2mk^2 + M_pm^2k^2} = \frac{nM_p{}^3}{nm^3 + M_p{}^2m + M_pm^2} \tag{20}$$

So when n or the ratio M_p/m is large, the efficiency gain of DMRG-isPT is considerable. In our experience, n is usually dozens if only one state is targeted. When several states are targeted together, such as calculating excited states in the state-average DMRG method, approximately, n will be multiplied by the number of requested states.[30] However, though the time cost is saved, the memory cost is not changed if M_p equals M.

The DMRG-isPT algorithm is very easy to be implemented in the existing DMRG or MPS code, because only the diagonalization part needs to be slightly changed. Due to the considerable efficiency gain, we expect our DMRG-isPT algorithm can further enlarge the M value that the existing DMRG code can deal with. In the next section, we give two numerical calculation examples to confirm that this efficient perturbation calculation applied on a small active space is reliable.

3. BENCHMARKS

3.1. Acene Series. The acene series are a kind of quasi-one-dimensional conjugated system (Figure 2a). Because of the potential to be used in the organic electronic device, they have been widely investigated both in theoretical and experimental studies.[31−34] One interesting question is that whether the ground state will become triplet in the long acene limit due to the increasing diradical character. Density functional theory (DFT) calculations by Houk et al.[32] predicted there exists a singlet triplet crossover. However, the many quasi-degenerate frontier orbitals in this system will result in strong static correlation effect, therefore the standard DFT calculation may fail. Thus, correlated electronic structure method is required.

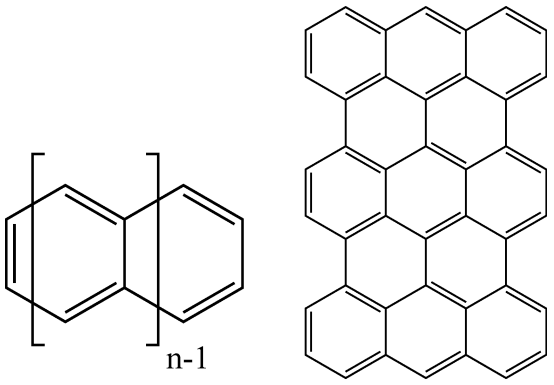

Figure 2. (a) Structure of [n]-acene. (b) Structure of [5,3]-periacene.

Hachmann et al.[33] performed ab initio DMRG calculation up to [12]-acene with single-ζ basis and up to [6]-acene with double-ζ basis. They predicted that in the infinite chain limit, the ground state remains singlet and the singlet−triplet gap is 8.69 ± 0.96 (STO-3G) and 3.33 ± 0.39 (DZ) kcal/mol. Other correlated electronic structure methods were also used to study this system[35,36] and they obtained the similar results for short chains. Chai et al.[34] calculated this system with thermally assisted-occupation density functional theory (TAO-DFT), revealing that there is no singlet triplet crossover up to [100]-acene and that the singlet−triplet gap is less than 1 kcal/mol in the infinite chain limit. Since DMRG has been proved to be very accurate in calculating such quasi-one-dimensional system, we aim to extend DMRG calculation to longer chains with model Hamiltonian.

The model Hamiltonian we choose is Pariser−Parr−Pople model (PPP).[37,38] It is the simplest but nontrivial chemical model Hamiltonian including long-range electron−electron interaction and is widely used in carbon-based conjugated polymers. The Hamiltonian is as follows:

$$\hat{H} = \sum_{i\sigma} \epsilon_i \hat{a}^\dagger_{i\sigma}\hat{a}_{i\sigma} + \sum_{\{ij\}\sigma} t_{ij}\hat{a}^\dagger_{i\sigma}\hat{a}_{j\sigma} + \sum_i U_i\hat{n}_{i\uparrow}\hat{n}_{i\downarrow} + \sum_{i<j} V_{ij}(\hat{n}_i - Z_i)(\hat{n}_j - Z_j) \tag{21}$$

The first term and the second term represent the site energy and nearest neighbor hopping. The third term is the Hubbard term representing the on-site Coulomb repulsion, and the last term represents the long-range Coulomb interaction. All the parameters we adopt here are the same as those used in ref 39. U_i = 11.26 eV and t_{ij} = −2.40 eV are the standard values for a conjugated carbon system, and the site energy differences are neglected. The long-range Coulomb potential V_{ij} is calculated with Ohno−Klopman analytical formula:[40,41]

$$V_{ij} = \frac{1}{\sqrt{4/(U_i + U_j)^2 + R_{ij}{}^2}} \tag{22}$$

The carbon−carbon bond length was fixed at 1.397 Å and set to be uniform for all the bonds. We calculate the acene chains from [2]-acene to [32]-acene and the maximum number of orbitals is 130. Since DMRG can achieve very accurate result with a small M in such quasi-one-dimensional system, we calculate the lowest singlet and triplet state by DMRG-isPT2/3 with two parameter conditions, one is (m = 256, M_p = 1024), the other is (m = 512, M_p = 1024). Meanwhile, we take the M = 1024 standard DMRG calculation as a reference. We calculate the lowest energy state in the S_z = 0 and S_z = 1 subspace respectively, and calculate the expectation value of $\hat{S}^2$ to identify the total spin of these two states.

In Figure 3, we present the energy error of the lowest singlet and triplet state as a function of acene length. Figure 3a shows the (m = 256, M_p = 1024) result, and Figure 3b shows the (m = 512, M_p = 1024) result. The M = 256 and 512 standard DMRG calculation results are also plotted as a comparison. The energy error almost linearly increases with the system size. But the slope of standard DMRG is much larger than that of DMRG-isPT. Even without energy correction, PT0 (blue circle), the energy is also lower than the standard DMRG result. This is because that at each optimization step, the wave function is corrected in the large space, and after renormalization, more entanglement from the large perturbation space is folded to the

DOI: 10.1021/acs.jctc.6b00696
J. Chem. Theory Comput. 2016, 12, 4871−4878

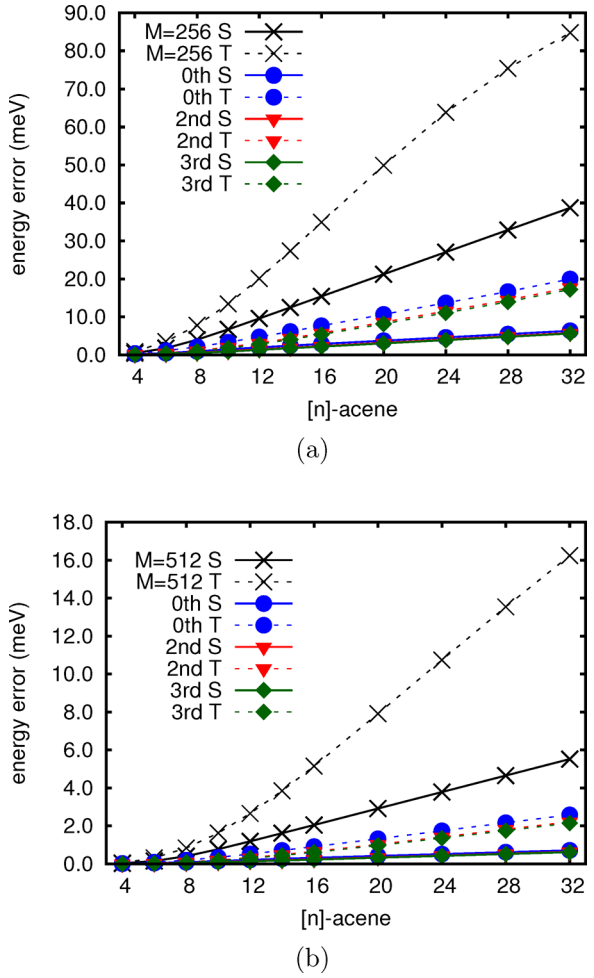

Figure 3. Energy error of the zeroth- (blue circle), second- (red triangle), and third-order (green diamond) corrected energy of the singlet (solid line) and triplet (dashed line) state of [n]-acene as a function of the number of acene rings n, calculated using DMRG-isPT2/3: (a) (m = 256, M = 1024), (b) (m = 512, M = 1024). For comparison, the (a) M = 256 and (b) M = 512 standard DMRG calculation results (cross) are also plotted. All results take the M = 1024 standard DMRG calculation result as a reference.

small active space. This is a feedback effect from the perturbation space. Therefore, the active space is more representative than standard DMRG in which the outer space is completely neglected. This confirms that the correlation effect of the outer space can be incorporated at this perturbation level. The second order energy correction lowers the total energy a lot (PT2, red triangle), especially in the triplet state case. Because of the high accuracy in this quasi-one-dimensional system, the third order energy correction (green diamond) can not be clearly seen in this figure. But in fact, it further lowers the total energy a little bit, indicating that the perturbation calculation converges well. Besides, the DMRG-isPT2/3 energy is always the upper bound of the true energy in these calculations (the energy error is positive), even though PT does not guarantee it. When half of the basis states belong to the active space, (m = 512, M_p = 1024) case, the accuracy loss is less than 1 meV for the singlet state and 2 meV for the triplet state, which is 1 order of magnitude improvement compared with the M = 512 standard DMRG calculation.

In Figure 4, we plot the singlet−triplet gap as a function of the acene length. The results are compared with the available

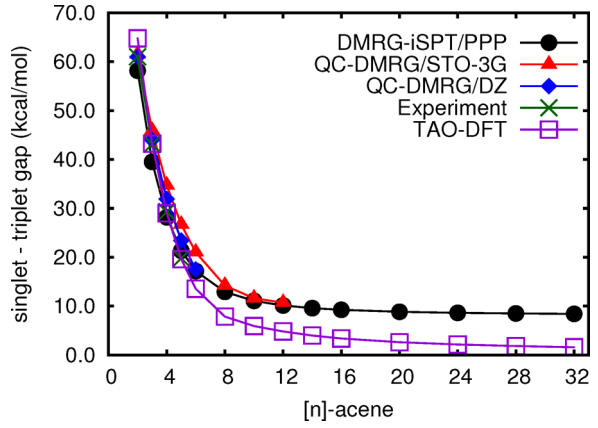

Figure 4. Singlet−triplet energy gap of [n]-acene as a function of the number of acene rings n, calculated using DMRG-isPT3. For comparison, the experimental data,[42−45] QC-DMRG data in STO-3G and DZ basis,[33] and TAO-DFT data[34] taken from the literature are also plotted.

experimental data,[42−45] ab initio DMRG results[33] and TAO-DFT results.[34] It shows that the DMRG-isPT result is reliable and consistent with the existing experimental data and ab initio DMRG results, but larger than TAO−DFT results, especially in the long chain acenes. The singlet−triplet gap decreases monotonically with the increase of acene length and it is 8.41 kcal/mol in [32]-acene. We also extrapolate from our data into the infinite polyacene limit and we find that the function $y = A_1 \exp{-x/t_1} + A_2 \exp{-x/t_2} + y_0$ can fit well and the adjusted R^2 is nearly 1. With this empirical function, the singlet−triplet gap in the infinite chain limit is 8.30 kcal/mol.

3.2. (5,3)-Periacene. DMRG is very accurate in one-dimensional or quasi-one-dimensional system. As the acene series calculated above, hundreds of retained basis states can give accurate enough low-lying states. However, the real chemical system is in general two-dimensional or three-dimensional. Large M value is always necessary to obtain an accurate result or even a qualitatively correct result in some cases. Periacene is a kind of two-dimensional polycyclic aromatic hydrocarbons, viewed as a graphene fragment. Like the polyacene, these systems have strong polyradical character. Thus, correlated electronic structure method is required to treat the static correlation effect. Yanai et al.[46] calculated the (3,n)-periacene with ab initio DMRG and they confirmed that the polyradical character is strong in these systems. Here we choose (5,3)-periacene as our model system (Figure 2b) to test how DMRG-isPT2/3 performs in such two-dimensional molecule. The Hamiltonian is still PPP Hamiltonian, and the same parameters are adopted as the above acene series. The M_p we select here equals 2000 and the m varies from 600 to 1400. At each m value, we both use the standard DMRG (M = m) and DMRG-isPT2/3 method to calculate the lowest singlet and triplet state. All the results take the M = 2000 standard DMRG result as a reference.

The energy errors of the lowest singlet, triplet, and singlet−triplet gap as a function of the number of retained basis states (m) in the active space are shown in Figure 5. In both standard DMRG and DMRG-isPT calculation, the energy error of singlet and triplet state decreases exponentially with the increase of the number of retained basis states in the active space. But, at the same m value, the error of standard DMRG result (red plus) is nearly 1 order of magnitude larger than the

DOI: 10.1021/acs.jctc.6b00696
J. Chem. Theory Comput. 2016, 12, 4871−4878

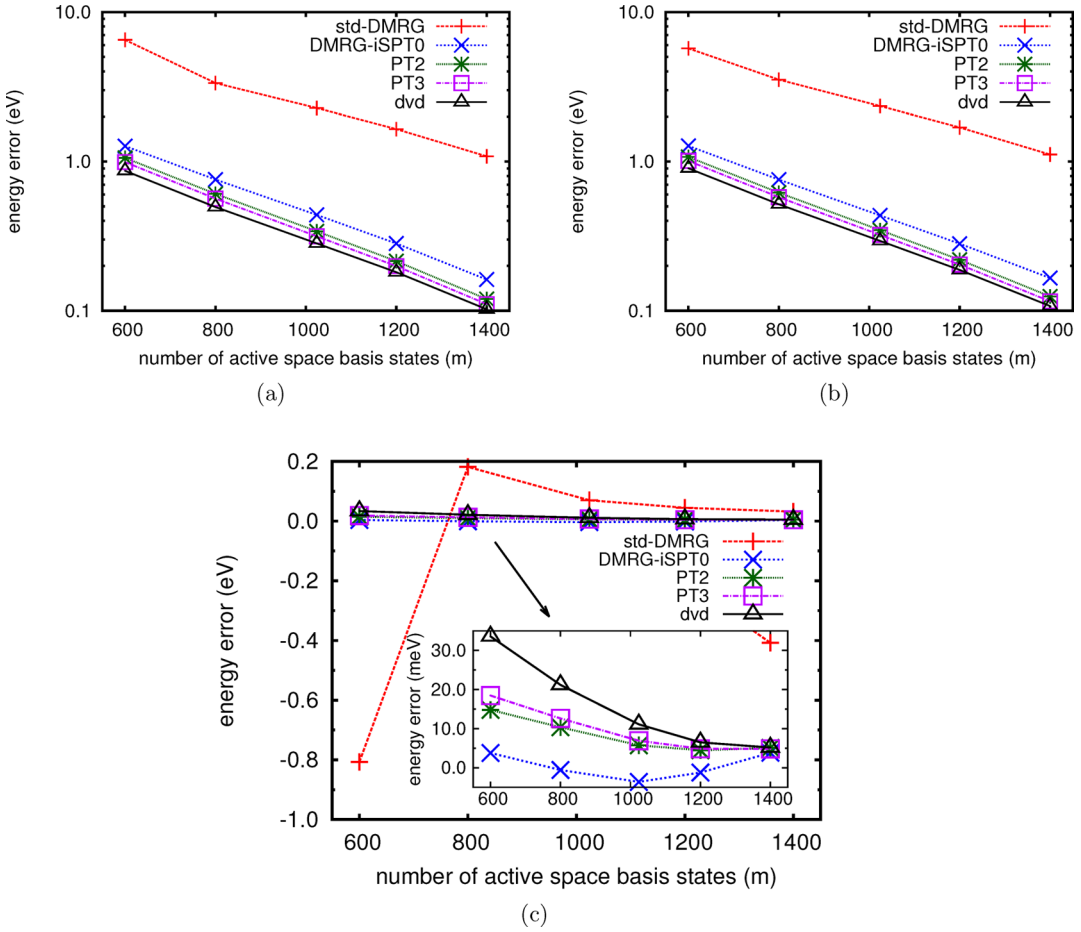

Figure 5. Energy error of the zeroth- (blue cross), second- (green star), third-order (magenta square), and last step exact diagonalization (black triangle) corrected energy of the (a) singlet and (b) triplet states and (c) singlet−triplet gap (the included figure is a zoom around 0 eV) of [5,3]-periacene as a function of the number of active space basis states (m), calculated using DMRG-isPT2/3. The Y-axis is presented in logarithmic scales. For comparison, the $M = m$ standard DMRG calculation results (red plus) are also plotted. All results take the $M = 2000$ standard DMRG calculation result as a reference.

other three perturbation corrected calculations, DMRG-isPT0, PT2 and PT3. From PT0 to PT3, the energy error decreases as expected. At the middle of each sweep, we also do exact diagonalization in the whole space and the result (dvd, black triangle) has a slight improvement compared with the PT3 result. With this exact diagonalization, we calculate the overlap between the exact eigenvector and the first order corrected wave function. It is larger than 0.99 in all cases. This confirms that the perturbation calculation is valid. Even without the energy correction, DMRG-isPT0 can achieve good improvement, which is similar to the acene series calculation. But in this two-dimensional system, this improvement is vital, especially in calculating the energy difference. In Figure 5c, the $M = 600$ standard DMRG calculation leads to a wrong energy level order, in which the lowest triplet state is 0.8 eV lower than the lowest singlet state. Only when we increase the M value, the energy level order can be corrected. But in our DMRG-isPT calculation, even in $m = 600$ case, the energy level order is correct and the gap error is less than 0.03 eV. This significant improvement proves that the entanglement from the outer space is important here and that perturbation treatment in DMRG-isPT is enough to include such entanglement effect. From the inset in Figure 5c, the gap error of DMRG-isPT0 is smaller than the other second or third order energy corrected result. We consider this is a result of the error cancellation. When the m value is large enough, the gap error could converge to 5 meV.

In summary, in such a simple two-dimensional molecule, when using our DMRG-isPT method, the energy error of one single state is 1 order of magnitude smaller than the standard DMRG result with $M = m$. Moreover, the energy level order is still correct even the active space is very small. When half of the retained basis states are included in the active space, the energy error of a single state is less than 0.3 eV and the error of relative energy is less than 0.02 eV.

With a proper wave function prediction algorithm,[47] the typical number of Davidson iterations n here is 20. The relative amounts of time spent at Davidson iteration in the standard DMRG calculation with different M value is shown in Table 1. It is over 90% in all cases as we expected. In the singlet state calculation, the speedup of DMRG-isPT3 for the whole DMRG sweep, compared to the M = 2000 standard DMRG calculation, is shown in Figure 6. Without further optimizing our code, the speedup varies between 6 and 2 from a small m to a large m.

Table 1. Relative Amounts of Time (%) Spent at Davidson Iteration in the Standard DMRG Algorithm

M	600	800	1024	1200	1400	2000
time	93.8	94.6	93.0	95.8	96.4	96.0

DOI: 10.1021/acs.jctc.6b00696
J. Chem. Theory Comput. 2016, 12, 4871−4878

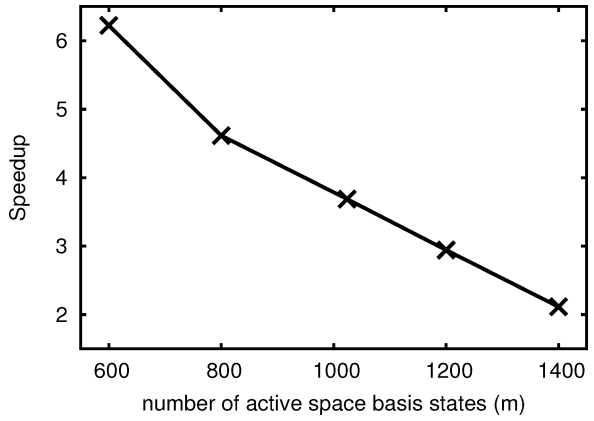

Figure 6. Speedup of the DMRG-isPT3 formulation (M_p = 2000) for the whole DMRG sweep as a function of the number of active space basis states. All calculations were performed on 2 Intel Xeon CPU E5-2640 v3 at 2.60 GHz.

Since in our numerical test, $m = \frac{1}{2}M_p$ is always a secure choice, the speedup could be more than 4. Besides, the speedup may increase if we target more than one state with the state-average algorithm.

4. CONCLUSIONS

In this work, we propose an inner space perturbation theory to optimize DMRG wave function (DMRG-isPT). We formulate an efficient algorithm that only one step Davidson iteration is required to calculate the first order wave function, the second and third-order energy. DMRG-isPT formulation takes advantage of the inherent nature of DMRG to increase the algorithm efficiency and at the same time to maintain the accuracy. Our numerical examples on the acene series and (5,3)-periacene show that the efficiency gain is considerable and that the accuracy loss due to the perturbation treatment is very small, when half of the total basis states belong to the active space. Thus, we can tackle with a larger M space now than standard DMRG, which is essential to treat two or three-dimensional system. We find that if M is small in standard DMRG, the space neglected by decimation is often important to reproduce correct singlet vs triplet state order in [5,3]-periacene. But the entanglement of such space can be incorporated with our DMRG-isPT method through an efficient perturbation calculation, and even DMRG-isPT0 can already achieve accurate results. Moreover, the perturbation corrected energy is always an upper bound of the true energy and converges in all our examples. Finally, We hope that this isPT formulation may be useful to other advanced tensor network states, such as TTNS. Because with this "small space diagonalization + large space perturbation" algorithm, TTNS can treat a large M efficiently and show its advantage over DMRG in more general systems.

AUTHOR INFORMATION

Corresponding Author

*E-mail: zgshuai@tsinghua.edu.cn.

Notes

The authors declare no competing financial interest.

ACKNOWLEDGMENTS

This work is supported by the National Natural Science Foundation of China (Grant no.21290191). Computational resources are supported by Tsinghua National Laboratory for Information Science and Technology.

REFERENCES

(1) White, S. R. *Phys. Rev. Lett.* **1992**, *69*, 2863.
(2) Shuai, Z.; Bredas, J.-L.; Pati, S. K.; Ramasesha, S. *Proc. SPIE* **1997**, *3145*, 293−302.
(3) Shuai, Z.; Pati, S. K.; Su, W.; Bredas, J.; Ramasesha, S. *Phys. Rev. B: Condens. Matter Mater. Phys.* **1997**, *55*, 15368.
(4) Fano, G.; Ortolani, F.; Ziosi, L. *J. Chem. Phys.* **1998**, *108*, 9246−9252.
(5) Marti, K. H.; Ondík, I. M.; Moritz, G.; Reiher, M. *J. Chem. Phys.* **2008**, *128*, 014104.
(6) Kurashige, Y.; Chan, G. K.-L.; Yanai, T. *Nat. Chem.* **2013**, *5*, 660−666.
(7) Sharma, S.; Sivalingam, K.; Neese, F.; Chan, G. K.-L. *Nat. Chem.* **2014**, *6*, 927−933.
(8) Clementi, E. Evolution of computers and simulations: From science and technology to the foundations of society. *Sci. China: Chem.* **2014**, *57* (10), 1317−1329.
(9) Sharma, S.; Chan, G. K.-L. *J. Chem. Phys.* **2012**, *136*, 124121.
(10) Wouters, S.; Poelmans, W.; Ayers, P. W.; Van Neck, D. *Comput. Phys. Commun.* **2014**, *185*, 1501−1514.
(11) Keller, S.; Dolfi, M.; Troyer, M.; Reiher, M. *J. Chem. Phys.* **2015**, *143*, 244118.
(12) Roos, B. O.; Taylor, P. R.; Sigbahn, P. E. *Chem. Phys.* **1980**, *48*, 157−173.
(13) Eisert, J.; Cramer, M.; Plenio, M. B. *Rev. Mod. Phys.* **2010**, *82*, 277.
(14) Wouters, S.; Nakatani, N.; Van Neck, D.; Chan, G. K.-L. *Phys. Rev. B: Condens. Matter Mater. Phys.* **2013**, *88*, 075122.
(15) Haegeman, J.; Osborne, T. J.; Verstraete, F. *Phys. Rev. B: Condens. Matter Mater. Phys.* **2013**, *88*, 075133.
(16) Murg, V.; Verstraete, F.; Legeza, Ö; Noack, R. *Phys. Rev. B: Condens. Matter Mater. Phys.* **2010**, *82*, 205105.
(17) Nakatani, N.; Chan, G. K.-L. *J. Chem. Phys.* **2013**, *138*, 134113.
(18) Davidson, E. R. *J. Comput. Phys.* **1975**, *17*, 87−94.
(19) Chan, G. K.-L. *J. Chem. Phys.* **2004**, *120*, 3172−3178.
(20) Møller, C.; Plesset, M. S. *Phys. Rev.* **1934**, *46*, 618.
(21) Andersson, K.; Malmqvist, P. A.; Roos, B. O.; Sadlej, A. J.; Wolinski, K. *J. Phys. Chem.* **1990**, *94*, 5483−5488.
(22) Kurashige, Y.; Yanai, T. *J. Chem. Phys.* **2011**, *135*, 094104.
(23) Sharma, S.; Chan, G. K.-L. *J. Chem. Phys.* **2014**, *141*, 111101.
(24) Guo, S.; Watson, M. A.; Hu, W.; Sun, Q.; Chan, G. K.-L. *J. Chem. Theory Comput.* **2016**, *12*, 1583−1591.
(25) Schollwöck, U. *Ann. Phys.* **2011**, *326*, 96−192.
(26) Chan, G. K.-L.; Head-Gordon, M. *J. Chem. Phys.* **2002**, *116*, 4462−4476.
(27) Chan, G. K.-L.; Sharma, S. *Annu. Rev. Phys. Chem.* **2011**, *62*, 465−481.
(28) Xiang, T. *Phys. Rev. B: Condens. Matter Mater. Phys.* **1996**, *53*, R10445.
(29) Helgaker, T.; Jorgensen, P.; Olsen, J. *Molecular electronic-structure theory*; John Wiley & Sons, 2000.
(30) Ma, H.; Ren, J.; Shuai, Z. *Zhongguo Kexue: Huaxue* **2015**, *45*, 1316.
(31) Bendikov, M.; Wudl, F.; Perepichka, D. F. *Chem. Rev.* **2004**, *104*, 4891−4946.
(32) Houk, K.; Lee, P. S.; Nendel, M. *J. Org. Chem.* **2001**, *66*, 5517−5521.
(33) Hachmann, J.; Dorando, J. J.; Avilés, M.; Chan, G. K.-L. *J. Chem. Phys.* **2007**, *127*, 134309.
(34) Wu, C.-S.; Chai, J.-D. *J. Chem. Theory Comput.* **2015**, *11*, 2003−2011.

DOI: 10.1021/acs.jctc.6b00696
J. Chem. Theory Comput. 2016, 12, 4871−4878

(35) Hajgató, B.; Szieberth, D.; Geerlings, P.; De Proft, F.; Deleuze, M. *J. Chem. Phys.* **2009**, *131*, 224321.
(36) Pelzer, K.; Greenman, L.; Gidofalvi, G.; Mazziotti, D. A. *J. Phys. Chem. A* **2011**, *115*, 5632−5640.
(37) Pople, J. *Trans. Faraday Soc.* **1953**, *49*, 1375−1385.
(38) Pariser, R.; Parr, R. G. *J. Chem. Phys.* **1953**, *21*, 466−471.
(39) Raghu, C.; Pati, Y. A.; Ramasesha, S. *Phys. Rev. B: Condens. Matter Mater. Phys.* **2002**, *66*, 035116.
(40) Ohno, K. *Theor. Chim. Acta* **1964**, *2*, 219−227.
(41) Klopman, G. *J. Am. Chem. Soc.* **1964**, *86*, 4550−4557.
(42) Birks, J. B. *Photophysics of aromatic molecules*; Wiley: London, 1970.
(43) Schiedt, J.; Weinkauf, R. *Chem. Phys. Lett.* **1997**, *266*, 201−205.
(44) Sabbatini, N.; Indelli, M.; Gandolfi, M.; Balzani, V. *J. Phys. Chem.* **1982**, *86*, 3585−3591.
(45) Burgos, J.; Pope, M.; Swenberg, C. E.; Alfano, R. *Phys. Status Solidi B* **1977**, *83*, 249−256.
(46) Mizukami, W.; Kurashige, Y.; Yanai, T. *J. Chem. Theory Comput.* **2013**, *9*, 401−407.
(47) White, S. R. *Phys. Rev. Lett.* **1996**, *77*, 3633.

DOI: 10.1021/acs.jctc.6b00696
J. Chem. Theory Comput. 2016, 12, 4871−4878